



Contents lists available at ScienceDirect

Bioorganic & Medicinal Chemistry Letters

journal homepage: www.elsevier.com/locate/bmcl

Acetazolamide-based [^{18}F]-PET tracer: *In vivo* validation of carbonic anhydrase IX as a sole target for imaging of CA-IX expressing hypoxic solid tumors

Kunal N. More^{a,1}, Jun Young Lee^{b,1}, Dong-Yeon Kim^c, Nam-Chul Cho^d, Ayoung Pyo^c, Misun Yun^c, Hyeon Sik Kim^c, Hangun Kim^a, Kwangseok Ko^d, Jeong-Hoon Park^{b,*}, Dong-Jo Chang^{a,*}

^a College of Pharmacy and Research Institute of Life and Pharmaceutical Sciences, Suncheon National University, Suncheon 57922, Republic of Korea

^b Radiation Instrumentation Research Division, Korea Atomic Energy Research Institute, Jeongseup 56212, Republic of Korea

^c Department of Nuclear Medicine, Chonam National University, Hwasun Hospital, Hwasun 58128, Republic of Korea

^d C&C Research Laboratories, DRC, Sungyunkwan University, Suwon 16419, Republic of Korea

ARTICLE INFO

Article history:

Received 12 September 2017

Revised 25 January 2018

Accepted 28 January 2018

Available online xxxxx

Keywords:

Carbonic anhydrase IX

Acetazolamide

Hypoxic tumor

PET imaging

Target validation

ABSTRACT

Carbonic anhydrase IX is overexpressed in many solid tumors including hypoxic tumors and is a potential target for cancer therapy and diagnosis. Reported imaging agents targeting CA-IX are successful mostly in clear cell renal carcinoma as SKRC-52 and no candidate was approved yet in clinical trials for imaging of CA-IX. To validate CA-IX as a valid target for imaging of hypoxic tumor, we designed and synthesized novel [^{18}F]-PET tracer (**1**) based on acetazolamide which is one of the well-known CA-IX inhibitors and performed imaging study in CA-IX expressing hypoxic tumor model as 4T1 and HT-29 *in vivo* models other than SKRC-52. [^{18}F]-acetazolamide (**1**) was found to be insufficient for the specific accumulation in CA-IX expressing tumor. This study might be useful to understand *in vivo* behavior of acetazolamide PET tracer and can contribute to the development of successful PET imaging agents targeting CA-IX in future. Additional study is needed to understand the mechanism of poor targeting of CA-IX, as if CA-IX is not reliable as a sole target for imaging of CA-IX expressing hypoxic solid tumors.

© 2018 Elsevier Ltd. All rights reserved.

Tumor hypoxia is a salient feature of broad numbers of solid tumors including frequent observations in distant metastasis. Hypoxic tumors with low level of O_2 below 20 mmHg are more prone to aggressive nature with poor prognosis, resistance to cancer therapy and low survival rate of cancer patients.^{1,2} Moreover, hypoxic cells are more resistant to radiation and chemotherapy than normoxic cells.³ Thus, hypoxia becomes a sign of advanced stage tumor; detection of which might be helpful to locate the tumor site. Recent discovery suggested many biomarkers for detection of hypoxic tumors microenvironment such as HIF-1 for cellular processes, vascular endothelial growth factor (VEGF) for angiogenesis, carbonic anhydrase IX (CA-IX) for pH regulation, and glucose transporter 1 (GLUT-1) for metabolism.⁴

CA-IX is a highly active cell surface anchored enzyme involved in hypoxia-induced stress, and is regulated by transcription factor, hypoxia-inducible factor-1 α (HIF-1 α) activated in response to

tumor hypoxia.^{2,5} Hypoxia-induced stabilization of HIF-1 α causes the expression of gene for CA-IX enzyme which alters cell homeostasis and consequently induces various oncogenic processes such as cell proliferation, angiogenesis, cell invasion, metastasis and metabolic changes in hypoxic tumors.^{6,7} Among 15 human isozymes of carbonic anhydrase (CA), CA-IX is a most active CA for the CO_2 hydration reaction and prominently overexpressed in hypoxic tumors.⁸ Overexpression of CA-IX plays a pivotal role in many cancers as non-small cell lung cancer (NSCLC),⁹ breast,^{10,11} renal cancer,¹² ovarian,¹³ brain,¹⁴ colon, and head and neck cancers.^{13,15} Expression of CA-IX in different cancers with featured hypoxia and presence of extracellular active site make it a promising target for anticancer therapy as well as an attractive target for drug delivery purpose such as imaging and therapy.¹⁶ The crystal structure of CA-IX enables to develop potent and selective small molecule inhibitors targeting CA-IX. Structurally, carbonic anhydrase is a metalloenzyme, and the active site is formed as distorted tetrahedral geometry with zinc ion as center in coordination with three imidazole groups of histidines and one hydroxide ion of substrate.¹⁷ Recent paradigm in cancer therapeutics is the development of new CA-IX inhibitors for better efficacy in alone or in

* Corresponding authors.

E-mail addresses: parkjh@kaeri.re.kr (J.-H. Park), djchang@sunchon.ac.kr (D.-J. Chang).

¹ The first two authors contributed equally to this work.

<https://doi.org/10.1016/j.bmcl.2018.01.060>

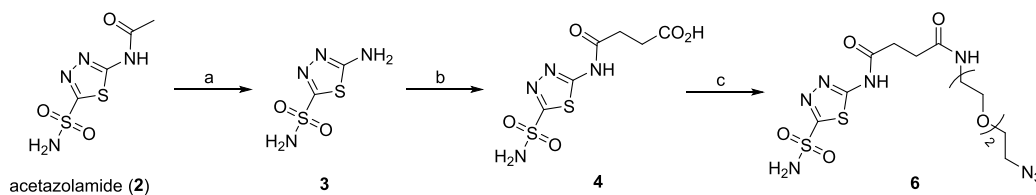
0960-894X/© 2018 Elsevier Ltd. All rights reserved.

combination with chemotherapeutic agent or radiotherapy.^{7,18,19} Small molecules inhibitors targeting CA-IX are either coumarin suicidal inhibitors or sulfonamides moiety.^{13,20,21} Sulfonamide ligand with high affinity to central metal ion of an enzyme can be utilized for the targeted delivery of potent cytotoxic drugs into solid tumors, which is otherwise showed ineffective biodistribution to desired tumor site and accumulated in normal tissues.^{19,22} Development of CA-IX inhibitors as an anticancer agent also enhanced the development of PET imaging ligand for diagnostics and small molecule-drug conjugates (SMDCs) for therapeutic purpose in both solid and metastatic tumors. Acetazolamide, a prototype²³ of sulfonamides, is a clinically approved *pan*-CA inhibitor with good profile,^{21,24} and is also known to possess antitumor activity alone or in combination.^{18,25} Suppression of tumor metastasis in lung carcinoma was also acquired by acetazolamide.²⁶ ^{99m}Tc-labeled acetazolamide was even used as a ligand for development of PET imaging radiotracer for imaging purpose²⁷ and SMDCs with acetazolamide ligand for pharmacodelivery of cytotoxic drug at tumor site.²⁸ However, most of the known radiotracers for imaging CA-IX as ^{99m}Tc-labeled acetazolamide ligand, ¹²⁴I-cG250 or ¹²⁴I- and ⁸⁹Zr-labeled antiCA-IX monoclonal antibodies were performed well predominantly for *in vivo* imaging of CA-IX in hypoxia independent renal cell carcinoma SKRC-52,^{27,29} even though CA-IX is also expressed in various hypoxic tumor models.³⁰ Only few PET tracer as ⁶⁸Ga-NOTGA-(AEBSA)₃ and ¹⁸F-AmBF3-(ABS)₃ with trimeric sulfonamide moieties achieved the proposed role. Surprisingly, the tracer with trimeric sulfonamide moieties showed higher uptake with selective targeting to CA-IX compared to monomeric and dimeric isoforms.²² Reported studies raised a question that CA-IX is really a universal target for imaging of all solid tumors other than SKRC-52. One review was published performing validation of CA-IX target for hypoxic tumor imaging.³¹ The review proposed that CA-IX is an unreliable target for hypoxic imaging due to the facts that CA-IX expression is cancer type-dependent, not all hypoxic tumors express CA-IX, expression of CA-IX is undetectable

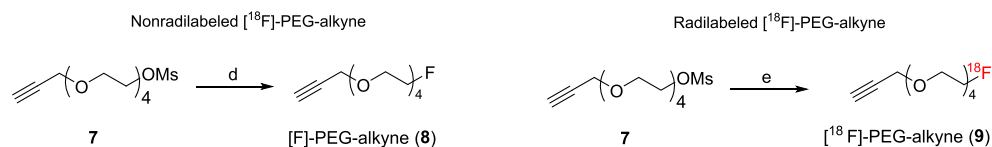
in certain cancer types, and re-oxygenation of previously hypoxic cancer cells induces expression of CA-IX. However, no *in vivo* experimental study was carried out to support this conclusion yet. Thus, further validation of CA-IX as a target for development of clinically feasible hypoxia imaging PET tracer is required to be performed. In the view of validation of CA-IX target for hypoxic tumor imaging, we designed and synthesized a new [¹⁸F]-PET tracer (**1**) based on acetazolamide as shown in Scheme 1. *In vivo* PET imaging and biodistribution studies of [¹⁸F]-PET tracer (**1**) were performed in CA-IX positive 4T1 and HT-29 skin xenograft Balb/c mice tumor models. 4T1 and HT-29 cancer cells are known to express CA-IX within hypoxic microenvironment. Imaging of PET tracer was also performed in CA-IX expressed lung metastatic tumors model formed by 4T1 breast cell lines.¹¹ The *in vivo* PET images and biodistribution profile provided insight about the behavior of our novel PET tracer [¹⁸F]-acetazolamide (**1**) on tumor model.

The precursor **6** for [¹⁸F]-labeling was synthesized to couple with [¹⁸F]-PEG-alkyne (**9**) to form central triazole ring by copper (I)-catalyzed click chemistry as shown in Scheme 1. The precursor **6** was synthesized starting with hydrolysis of commercially available acetazolamide (**2**) giving compound **3**. Compound **3** was reacted with succinic anhydride in DMF with heating to obtain carboxylic acid (**4**). Compound **4** was subjected to amide coupling reaction with azide-PEG linker (2-(2-(2-azidoethoxy)ethoxy)ethan-1-amine) (**5**) using BOP which finally provided the precursor (**6**) for click reaction. This precursor was then used for synthesis of radiolabeled [¹⁸F]-acetazolamide (**1**) through the click reaction with [¹⁸F]-PEG-alkyne (**9**). Radiolabeling of the mesylated PEG-alkyne linker (**7**) successfully provided [¹⁸F]-PEG-alkyne precursor (**9**) in 32.5% radiochemical yield with >99% of radiochemical purity. The click reaction of precursor (**6**) with [¹⁸F]-PEG-alkyne (**9**) was performed to obtain final [¹⁸F]-PET tracer (**1**) in radiochemical yield of 93.73% and radiochemical purity >99% after HPLC purification (see Fig. S1 and Table S1, ESI†).

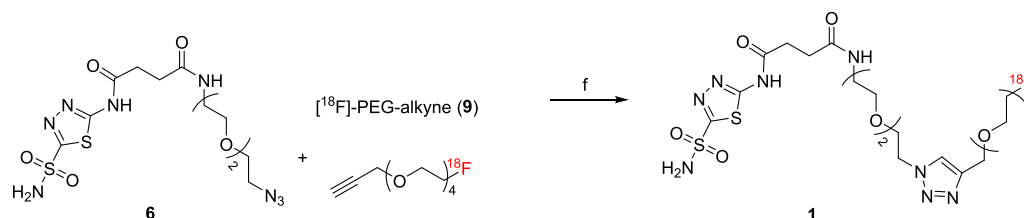
A. Synthesis of precursor 6 for click reaction



B. Fluorination reaction: Synthesis of precursor 8 and 9 for click reaction



C. Click reaction



Scheme 1. Reaction conditions and reagents: A. (a) conc. HCl, EtOH, reflux, quant. yield; (b) succinic anhydride, DMF, 100 °C, 96%; (c) 2-(2-(2-azidoethoxy)ethoxy)ethan-1-amine (**5**), BOP, *i*PrNEt₂, DMF, rt, 53%; B. (d) TBAF, THF, 80 °C, 33%; (e) ¹⁸F/[2,2,2]-cryptand, CH₃CN, 100 or 80 °C, 33%; C. (f) CuI, *i*PrNEt₂, CH₃CN, rt, 94%.

PET imaging was performed after tail *i.v.* injection of [^{18}F]-acetazolamide (**1**) inside CA-IX expressing 4T1 and HT-29 skin xenograft tumor models to investigate the efficiency of PET tracer for its uptake to tumor. (Fig. 1A and B) *In vivo* PET imaging scans were performed over different time interval such as 5, 15, 30, 60 and 90 min. Initially, the strong signal was detected in abdomen, intensity of which was decreased over time at final scans. MicroPET imaging study of [^{18}F]-acetazolamide (**1**) showed undetectable uptake in 4T1 and HT-29 xenograft tumors against background tissues. This PET imaging study was performed at different time points p.i. to see the variation in uptake level of [^{18}F]-acetazolamide (**1**) into tumors over the time. Unfortunately, not a single time point shows any detectable amount in tumor, suggesting that PET tracer (**1**) is not specifically accumulated in CA-IX expressing tumor.

In order to understand the fate of [^{18}F]-acetazolamide (**1**) inside the CA-IX expressed mice body, biodistribution study was performed after harvesting various body organs. (Fig. 2A and B) In this study, the mouse blood sample was obtained by heart puncture and then heart, lung, liver, spleen, stomach, intestine, pancreas, kidney, muscle, fat, bone, skin, tail, tumor, and brain were harvested, weighed and counted by using gamma counter at each time interval at 15, 30, 60 and 90 min. [^{18}F]-Acetazolamide (**1**) was localized in tumor with very trace amount but most is accumulated in intestine in both cases of tumor types. Kidney and stomach were also shown detectable signal which diminished over the time. Tumor model with HT-29 cells, when compared to 4T1 xenograft, retained more amount of PET in blood compared to tumor. The high blood uptake in HT-29 might be due to binding to CA-II in red blood cell. In case of 4T1 xenograft, intestinal amount of

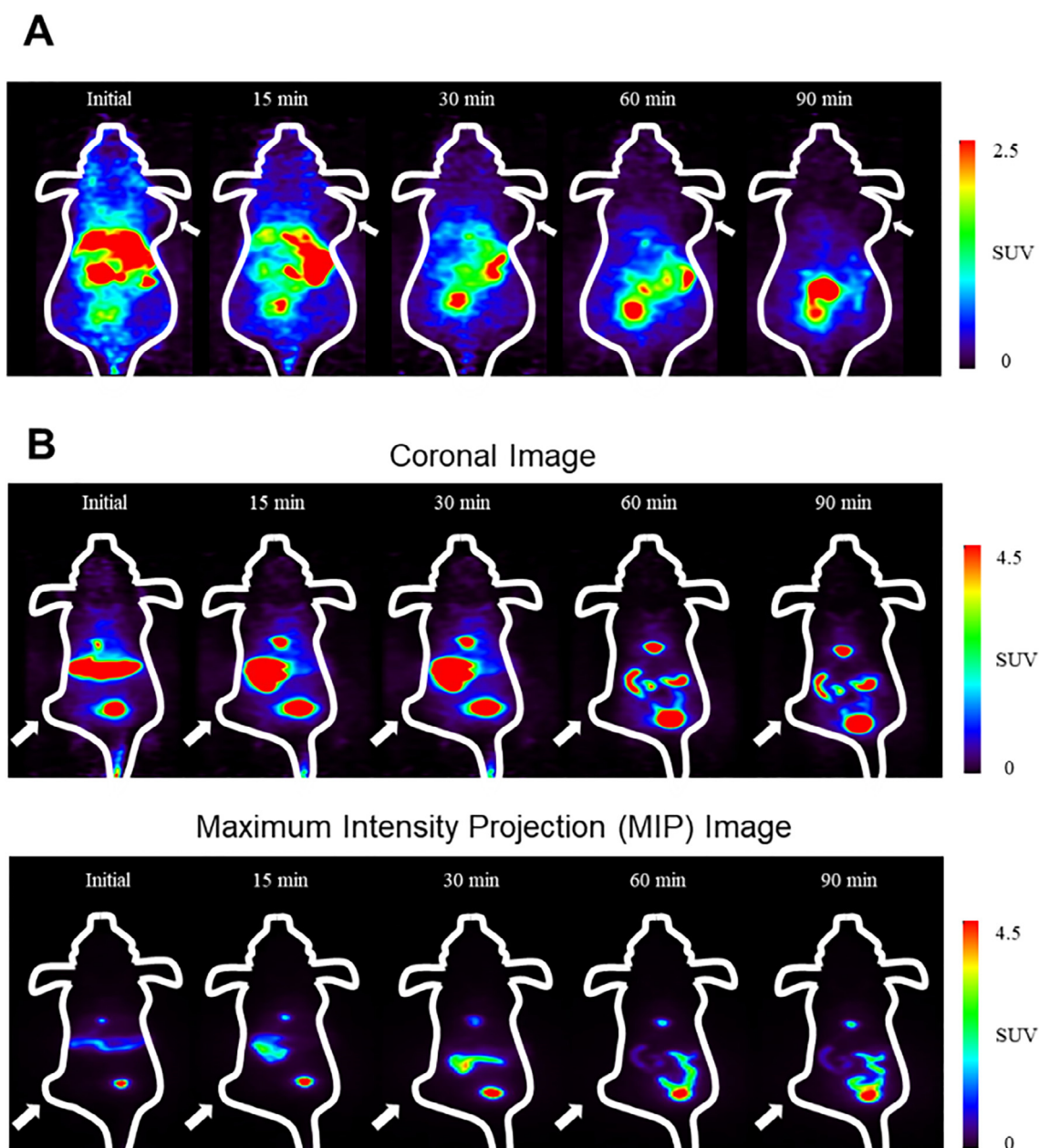


Fig. 1. A. MicroPET images of Balb/C mice xenograft bearing 4T1 cells at 5, 15, 30, 60 and 90 min. B. Coronal microPET images (top) and maximum intensity projection (bottom) microPET images of Balb/C mice bearing HT-29 cells at 5, 15, 30, 60 and 90 min. Tumor positions are indicated by white arrows.

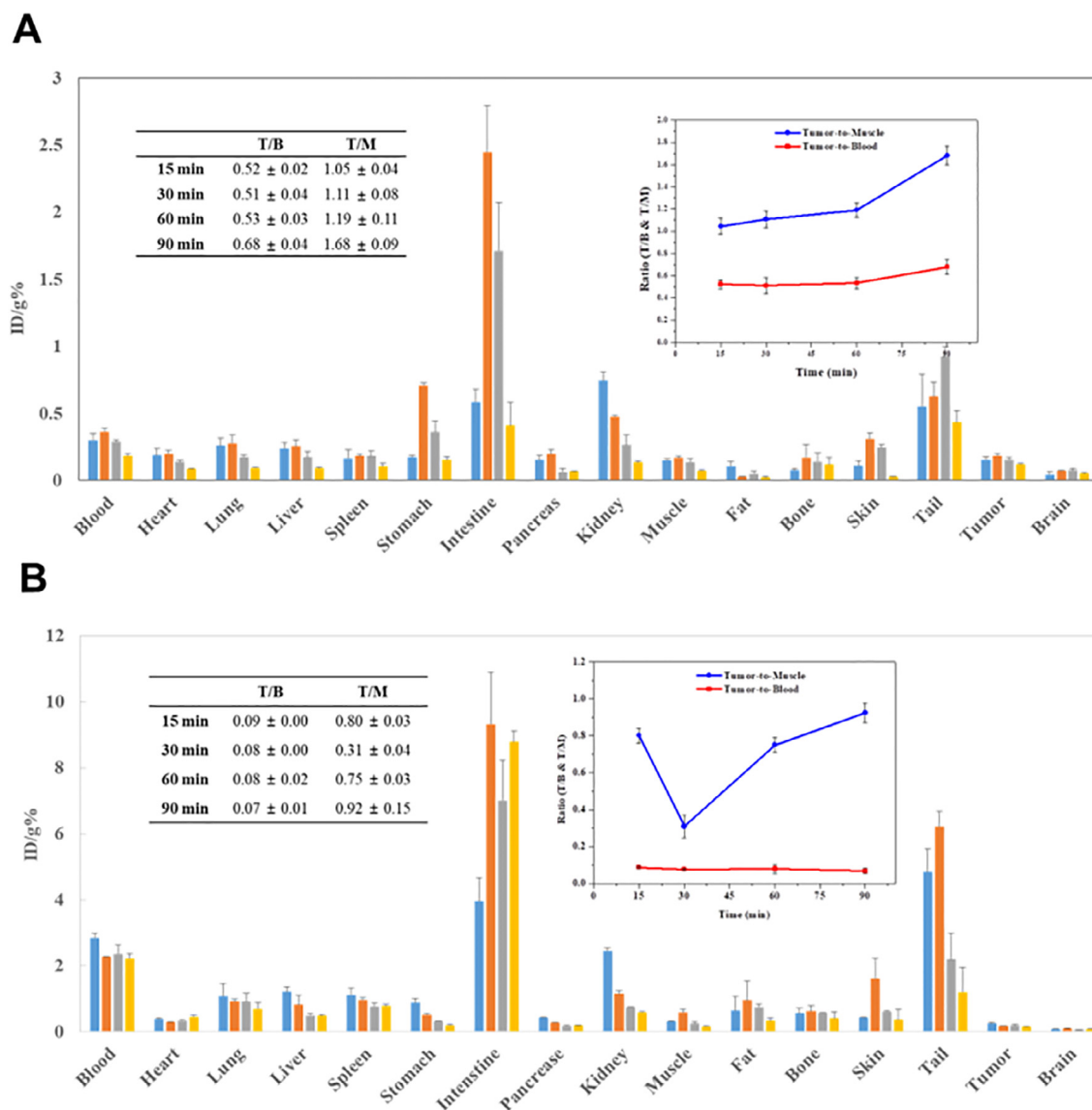


Fig. 2. Biodistribution study of [^{18}F]-acetazolamide (**1**). A. On Balb/C xenograft model bearing 4T1 cells at 15, 30, 60 and 90 min. B. On Balb/C xenograft model bearing HT-29 cells at 15, 30, 60, and 90 min.

[^{18}F]-acetazolamide (**1**) decreased over time showing fast clearance rate from intestine, whereas in HT-29 most amount accumulated in intestine for longer time, and only trace amount of PET tracer was passed to tumor. Tumor to blood and tumor to muscle ratio of tracer in 4T1 xenograft didn't show any change over time suggesting inefficient uptake in tumor. It was confirmed that [^{18}F]-acetazolamide (**1**) was accumulated highly in intestine in HT-29 and 4T1 xenografts and no signal was found in both tumor models, which concluded that [^{18}F]-acetazolamide (**1**) is not targeted well to CA-IX tumor.

CA-IX is a vital biomarker for tumor progression and metastatic tumors, and hypoxia-dependent CA-IX expression has been known to induce the metastasis in progress of cancer.¹¹ Metastasis tumors are more challenging to manage clinically,³² thus CA-IX imaging would be a great importance in metastatic tumors. To evaluate feasibility of CA-IX imaging in metastatic tumor, we performed the microPET study of [^{18}F]-acetazolamide tracer (**1**) in lung metastatic tumor models induced by 4T1 breast cancer cells as shown in Fig. 3. Intravenous injection of [^{18}F]-acetazolamide (**1**) in lung metastatic tumor model was not successful for detection of lung

metastases. The imaging scan showed no accumulation of PET tracer in metastatic lung tumor, with more accumulation in abdomen like xenograft tumor model even after 120 min.

The pharmacokinetic nature of [^{18}F]-acetazolamide (**1**) was assessed through the evaluation of partition coefficient, *in vitro* stability in human serum and *in vivo* stability in Balb/C mice. The log *p* value of -1.87 ± 0.0093 suggested the hydrophilic nature of [^{18}F]-acetazolamide (**1**) (see Table S1, ESI[†]). Hydrophilic tracers have some advantages as less prone to blood protein binding allowing high fraction of a free drug, which leads the drug permeation to reach tissues, and faster clearance kinetics with low toxicity. As shown in Fig. 4, [^{18}F]-acetazolamide (**1**) was found to be almost 81% intact in human serum after 90 min (also see Table S2, ESI[†]). *In vivo* stability study of [^{18}F]-Acetazolamide in Balb/C mice showed that 50% of the PET tracer was intact after 30 min with decreasing stability with 20% at 1hr and 10% after 2hr post injection (see Table S3, ESI[†]). The low signal in bone (Fig. 2) suggested that the decreased stability of [^{18}F]-acetazolamide (**1**) is due to the metabolic degradation by a process other than defluorination of [^{18}F] fluoride.³³ However, the low tumor uptake in PET imaging

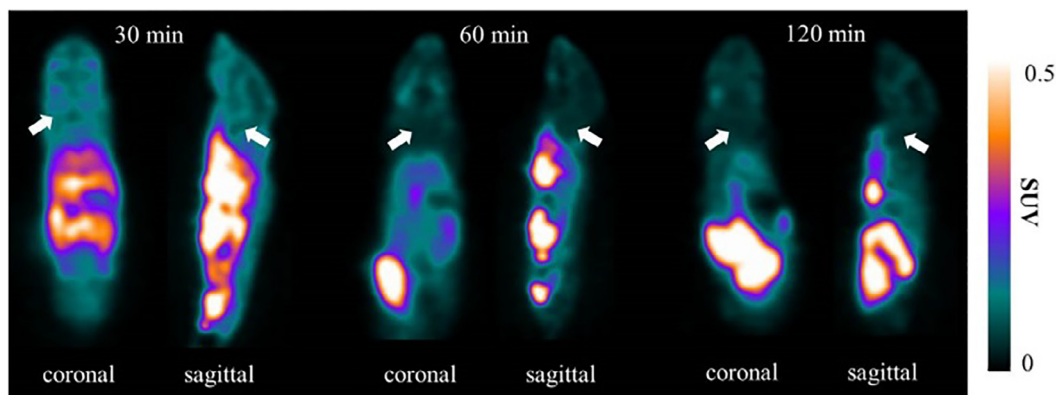


Fig. 3. MicroPET images of [^{18}F]-acetazolamide (**1**) in lung metastatic tumor model induced by 4T1 cells at time interval of 30 min, 60 min and 120 min. Tumor positions are indicated by white arrows.

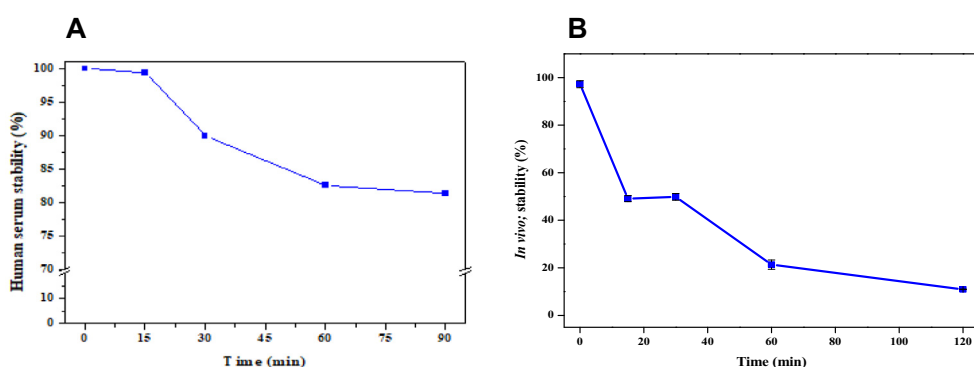


Fig. 4. Stability of [^{18}F]-acetazolamide (**1**). A. *In vitro* stability in human serum. B. *In vivo* stability in 8 weeks old Balb/C mice.

does not come from the result of *in vitro* and *in vivo* instability because almost 80% (90 min, *in vitro*) and 50% (30 min, *in vivo*) of PET tracer was intact for significant time span for imaging study, suggesting [^{18}F]-acetazolamide (**1**) is a feasible PET tracer for *in vivo* imaging.

Molecular docking study was performed to investigate whether [^{18}F]-acetazolamide (**1**) could bind to CA-IX. Binding parameters of our PET tracer were calculated using Schrödinger Suite program (Schrödinger LLC, NY, USA). The human CA-IX mimic co-crystal structure (PDB ID: 4K0S) with acetazolamide was used as a model structure for this docking study. The human CA-IX mimic, which is a CA-IX analogue engineered by site-specific mutations in the active site of CA-II, has been powerfully used for the development of carbonic anhydrase inhibitors.³⁴ Prior to the docking study of [^{18}F]-acetazolamide (**1**), the binding mode of acetazolamide was first predicted to confirm the accuracy of docking study by this modeling module. As shown in Fig. 5B, the binding mode of acetazolamide in docking study is the almost same as that of the X-ray co-crystal structure. Based on this result for acetazolamide, the docking study of [^{18}F]-acetazolamide (**1**) in the hCA-IX mimic crystal structure was conducted to investigate whether [^{18}F]-acetazolamide (**1**) has a similar binding mode to acetazolamide. As presented in Fig 5C and D, the predicted binding mode of [^{18}F]-acetazolamide (**1**) with the lowest binding scores (Gscore³⁵ \sim -7.96 kcal/mol and Emodel³⁶ \sim -101.38 kJ/mol), which were similar to those of acetazolamide (Gscore \sim -9.04 kcal/mol and Emodel \sim -79.19 kJ/mol), showed a good match for the binding conformation of co-crystallized acetazolamide. This precise analysis of the docking study suggested that [^{18}F]-acetazolamide (**1**) would probably exhibit

the similar binding affinity and can be a good ligand of CA-IX for imaging study.

Adams et al. reported that only 35% of human invasive breast cancers expressed CA-IX and not a single biomarker target serve as a sole target for imaging purpose.³⁷ Reason of inefficiency of [^{18}F]-acetazolamide (**1**) to detect the 4T1 breast cancer and its metastatic tumor need to be evaluated by additional study. HT-29 is a popular tumor model for development of CA-IX targeting tracer. But most of PET tracers are unsuccessful to accumulate in these tumors except tracers with trimeric structure to achieve strong affinity for CA-IX.²² No uptake of our synthesized probe [^{18}F]-acetazolamide (**1**) inside tumor in HT-29 xenograft model motivated to perform a separate detailed study. In conclusion, we successfully synthesized a novel [^{18}F] radiolabeled acetazolamide ligand and evaluated its potential as CA-IX targeted PET tracer. However, its uptake in both 4T1 and HT-29 tumors was minimal. The *in vivo* imaging study of [^{18}F]-acetazolamide (**1**) in this context showed that the synthesized acetazolamide-based PET tracer showed poor uptake in CA-IX expressed hypoxic tumor on skin xenograft and metastatic xenograft *in vivo* models. As mentioned earlier, CA-IX is overexpressed in many types of cancer, but most of imaging agents targeting CA-IX are mainly effective on *in vivo* model with specific cell lines such as SKRC-52 cells. This study and previous reports witnessed that CA-IX might not be reliable as sole universal target for imaging of CA-IX expressed hypoxic solid tumors although there was an exception with trimeric binding moiety for strong binding. Thus, an additional study is needed to confirm if the CA-IX is a good target for imaging of hypoxic tumor or our synthesized PET tracer was unable to

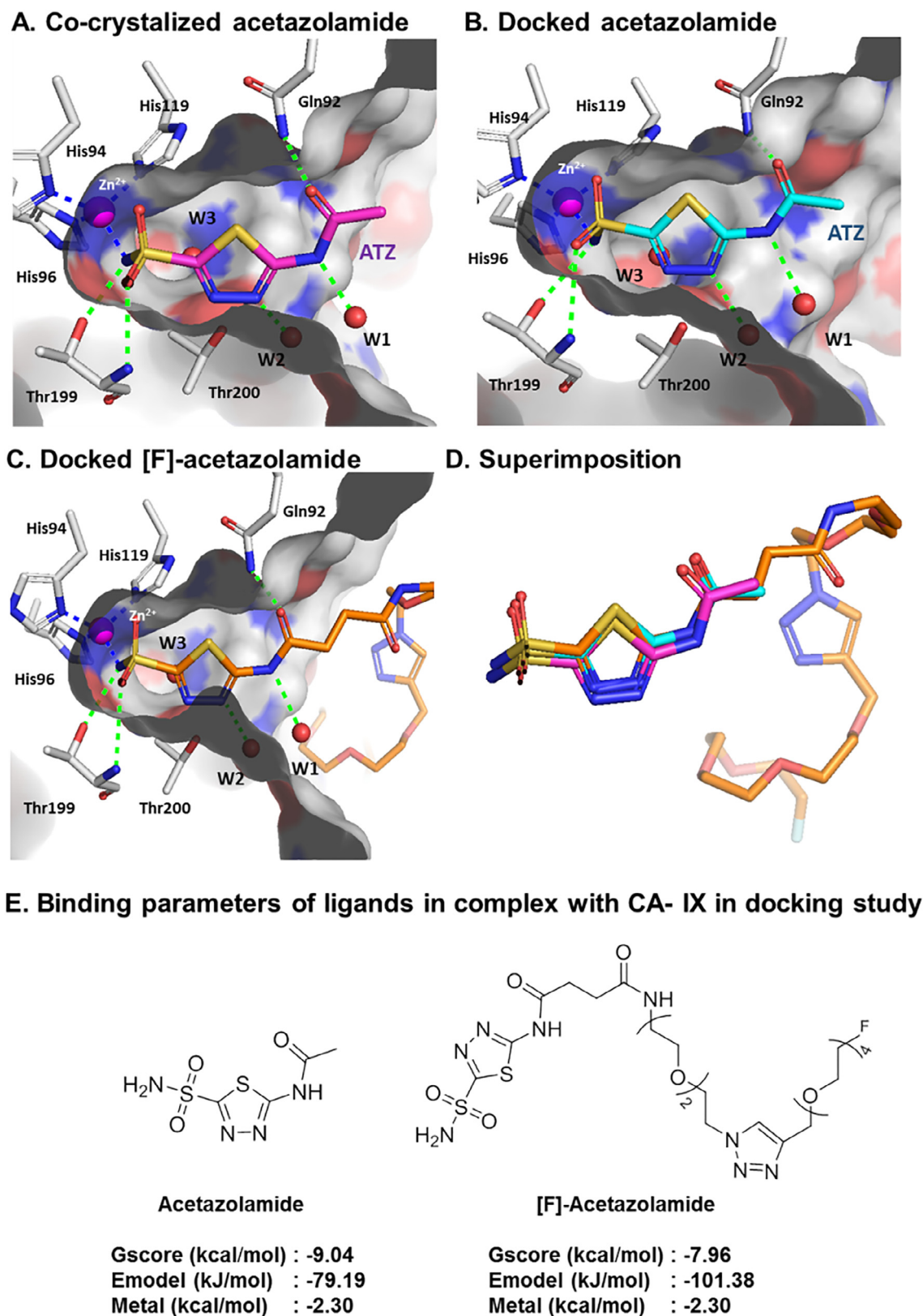


Fig. 5. Docking study of acetazolamide and [F]-acetazolamide (**1**) in the active site of human CA-IX mimic crystal structure (PDB ID 4K0S). A. X-ray co-crystal structure of acetazolamide, B. The predicted binding mode of acetazolamide, C. The predicted binding mode of [F]-acetazolamide (**1**), D. Superimposition of the predicted conformation of [F]-acetazolamide (**1**) with the co-crystallized acetazolamide, E. Binding parameters of acetazolamide and [F]-acetazolamide (**1**) in docking study. Molecular images were generated by PyMOL program. (Zn atom: violet sphere, Hydrogen bonds: green dot lines, the interactions with Zn: blue dot lines).

perform well in imaging study. The study performed in this context might aid to design new PET tracer which can successfully target CA-IX in hypoxic condition.

Acknowledgments

This work was supported by the National Research Foundation of Korea (NRF) funded by the Ministry of Science, ICT & Future Planning (NRF-2016M2C2A1937988, NRF-2016M2B2A4909218 & NRF-2017M2B2A4042384).

A. Supplementary data

Supplementary data associated with this article can be found, in the online version, at <https://doi.org/10.1016/j.bmcl.2018.01.060>.

References

- Harris AL. Hypoxia—a key regulatory factor in tumour growth. *Nat Rev Cancer*. 2002;2:38–47.
- Wykoff CC, Beasley NJP, Watson PH, et al. Hypoxia-inducible expression of tumor-associated carbonic anhydrases. *Cancer Res*. 2000;60:7075–7083.
- Wilson WR, Hay MP. Targeting hypoxia in cancer therapy. *Nat Rev Cancer*. 2011;11:393–410.
- (a) Krohn KA, Link JM, Mason RP. Molecular imaging of hypoxia. *J Nucl Med*. 2008;49:129S–148S; (b) Padhani AR, Krohn KA, Lewis JS, Alber M. Imaging oxygenation of human tumours. *Eur Radiol*. 2007;17:861–872; (c) Isa AY, Ward TH, West CML, Slevin NJ, Homer JJ. Hypoxia in head and neck cancer. *Br J Radiol*. 2006;79:791–798.
- Lendahl U, Lee KL, Yang H, Poellinger L. Generating specificity and diversity in the transcriptional response to hypoxia. *Nat Rev Genet*. 2009;10:821–832.
- Ivanov S, Liao SY, Ivanova A, et al. Expression of Hypoxia-Inducible Cell-Surface Transmembrane Carbonic Anhydrases in Human Cancer. *Am J Pathol*. 2001;158:905–919.
- Winum JY, Rami M, Scozzafava A, Montero JL, Supuran C. Carbonic anhydrase IX: a new druggable target for the design of antitumor agents. *Med Res Rev*. 2008;28:445–463.
- Hilvo M, Baranauksiene L, Salzano AM, et al. Biochemical characterization of CA IX, one of the most active carbonic anhydrase isozymes. *J Biol Chem*. 2008;283:27799–27809.
- Ilie M, Mazure NM, Hofman V, et al. High levels of carbonic anhydrase IX in tumour tissue and plasma are biomarkers of poor prognostic in patients with non-small cell lung cancer. *Br J Cancer*. 2010;102:1627–1635.
- Chia SK, Wykoff CC, Watson PH, et al. Prognostic significance of a novel hypoxia-regulated marker, carbonic anhydrase IX, in invasive breast carcinoma. *J Clin Oncol*. 2001;19:3660–3668.
- Lou Y, McDonald PC, Oloumi A, et al. Targeting tumor hypoxia: suppression of breast tumor growth and metastasis by novel carbonic anhydrase IX inhibitors. *Cancer Res*. 2011;71:3364–3376.
- (a) Bui MHT, Seligson D, Han KR, et al. Carbonic anhydrase IX is an independent predictor of survival in advanced renal clear cell carcinoma: implications for prognosis and therapy. *Clin Cancer Res*. 2003;9:802–811; (b) Stillebroer AB, Mulders PFA, Boerman OC, Oyen WJG, Oosterwijk E. Carbonic anhydrase IX in renal cell carcinoma: implications for prognosis, diagnosis, and therapy. *Eur Urol*. 2010;58:75–83.
- Supuran CT. Inhibition of carbonic anhydrase IX as a novel anticancer mechanism. *World J Clin Oncol*. 2012;3:98–103.
- (a) Jarvela S, Parkkila S, Bragge H, et al. Carbonic anhydrase IX in oligodendroglial brain tumors. *BMC Cancer*. 2008;8:1–9; (b) Harun MS, Claudiu TS, Carsten H, et al. Modulation of carbonic anhydrase 9 (CA9) in human brain cancer. *Curr Pharm Des*. 2010;16:3288–3299.
- Koukourakis MI, Giatromanolaki A, Sivridis E, et al. Hypoxia-regulated carbonic anhydrase-9 (CA9) relates to poor vascularization and resistance of squamous cell head and neck cancer to chemoradiotherapy. *Clin Cancer Res*. 2001;7:3399–3403.
- Potter CPS, Harris AL. Diagnostic, prognostic and therapeutic implications of carbonic anhydrases in cancer. *Br J Cancer*. 2003;89:2–7.
- (a) Krishnamurthy VM, Kaufman GK, Urbach AR, et al. Carbonic anhydrase as a model for biophysical and physical-organic studies of proteins and protein-ligand binding. *Chem Rev*. 2008;108:946–1051; (b) Alterio V, Hilvo M, Di Fiore A, et al. Crystal structure of the catalytic domain of the tumor-associated human carbonic anhydrase IX. *Proc Natl Acad Sci USA*. 2009;106:16233–16238.
- Ahlskog JKJ, Dumelin CE, Trussel S, Marling J, Neri D. In vivo targeting of tumor-associated carbonic anhydrases using acetazolamide derivatives. *Bioorg Med Chem Lett*. 2009;19:4851–4856.
- McDonald PC, Winum JY, Supuran CT, Dedhar S. Recent developments in targeting carbonic anhydrase IX for cancer therapeutics. *Oncotarget*. 2012;3:84–97.
- Neri D, Supuran CT. Interfering with pH regulation in tumours as a therapeutic strategy. *Nat Rev Drug Discov*. 2011;10:767–777.
- Supuran CT. Carbonic anhydrases: novel therapeutic applications for inhibitors and activators. *Nat Rev Drug Discov*. 2008;7:168–181.
- (a) Guan SS, Cheng CC, Ho AS, et al. Sulfonamide derivative targeting carbonic anhydrase IX as a nuclear imaging probe for colorectal cancer detection in vivo. *Oncotarget*. 2015;6:36139–36155; (b) Lau J, Zhang Z, Jenni S, et al. PET imaging of carbonic anhydrase IX expression of HT-29 tumor xenograft mice with 68Ga-labeled benzenesulfonamides. *Mol Pharm*. 2016;13:1137–1146; (c) Lau J, Liu ZZ, Pan J, et al. Trimeric 18F-AmBF3-sulfonamides for imaging carbonic anhydrase IX expression. *J Nucl Med*. 2015;56:557–557.
- (a) Mann T, Keilin D. Sulphanilamide as a specific inhibitor of carbonic anhydrase. *Nature*. 1940;146:164–165; (b) Roblin RO, Clapp JW. The Preparation of heterocyclic sulfonamides. *J Am Chem Soc*. 1950;72:4890–4892.
- Kassamali R, Sica DA. Acetazolamide: a forgotten diuretic agent. *Cardiol Rev*. 2011;19:276–278.
- Faes S, Planche A, Uldry E, et al. Targeting carbonic anhydrase IX improves the anti-cancer efficacy of mTOR inhibitors. *Oncotarget*. 2016;7:36666–36680.
- Xiang Y, Ma B, Li T, Yu HM, Li XJ. Acetazolamide suppresses tumor metastasis and related protein expression in mice bearing Lewis lung carcinoma. *Acta Pharmacol Sin*. 2002;23:745–751.
- Krall N, Pretto F, Mattarella M, Muller C, Neri D. A 99mTc-labeled ligand of carbonic anhydrase IX selectively targets renal cell carcinoma in vivo. *J Nucl Med*. 2016;57:943–949.
- (a) Krall N, Pretto F, Decurtins W, Bernardes GJL, Supuran CT, Neri D. A small-molecule drug conjugate for the treatment of carbonic anhydrase IX expressing tumors. *Angew Chem Int Ed*. 2014;53:4231–4235; (b) Cazzamalli S, Dal Corso A, Neri D. Acetazolamide serves as selective delivery vehicle for dipeptide-linked drugs to renal cell carcinoma. *Mol Cancer Ther*. 2016;15:2926–2935.
- (a) Lawrentschuk N, Lee FT, Jones G, et al. Investigation of hypoxia and carbonic anhydrase IX expression in a renal cell carcinoma xenograft model with oxygen tension measurements and 124I-cG250 PET/CT. *Urol Oncol*. 2011;29:411–420; (b) Stillebroer AB, Franssen GM, Mulders PFA, et al. ImmunoPET imaging of renal cell carcinoma with (124)I- and (89)Zr-labeled anti-CAIX monoclonal antibody cG250 in mice. *Cancer Biother Radiopharm*. 2013;28:510–515.
- (a) McDonald PC, Dedhar S. Carbonic anhydrase IX (CAIX) as a mediator of hypoxia-induced stress response in cancer cells. In: Frost SC, McKenna R, eds. *Carbonic anhydrase: mechanism, regulation, links to disease, and industrial applications*. Dordrecht: Springer, Netherlands; 2014:255–269; (b) Bao B, Groves K, Zhang J, et al. In vivo imaging and quantification of carbonic anhydrase IX expression as an endogenous biomarker of tumor hypoxia. *PLoS One*. 2012;7:e50860.
- Li J, Zhang G, Wang X, Li XF. Is carbonic anhydrase IX a validated target for molecular imaging of cancer and hypoxia? *Future Oncol*. 2015;11:1531–1541.
- Van Kuijk SJA, Yaromina A, Houben R, Niemans R, Lambin P, Dubois LJ. Prognostic significance of carbonic anhydrase IX expression in cancer patients: a meta-analysis. *Front Oncol*. 2016;6:69.
- Kuchar M, Mamat C. Methods to increase the metabolic stability of 18F-radiotracers. *Molecules*. 2015;20:16186–16220.
- Moeker J, Mahon BP, Bornaghi LF, et al. Structural insights into carbonic anhydrase IX isoform specificity of carbohydrate-based sulfamates. *J Med Chem*. 2014;57:8635–8645.
- Halgren TA, Murphy RB, Friesner RA, et al. Glide: a new approach for rapid, accurate docking and scoring. 2. Enrichment factors in database screening. *J Med Chem*. 2004;47:1750–1759.
- Friesner RA, Banks JL, Murphy RB, et al. Glide: a new approach for rapid, accurate docking and scoring. 1. Method and assessment of docking accuracy. *J Med Chem*. 2004;47:1739–1749.
- Adams A, van Brussel ASA, Vermeulen JF, et al. The potential of hypoxia markers as target for breast molecular imaging – a systematic review and meta-analysis of human marker expression. *BMC Cancer*. 2013;13:538–538.